J. Condensed Matter Nucl. Sci. 27 (2018) 22–29

Research Article

Increase of an Anti-Stokes Peak at the Cathode of an Electrically Driven, Active Aqueous Nickel/H_2O/Pt System

Mitchell R. Swartz*

JET Energy Inc., Wellesley Hills, MA 02481, USA

Abstract

Coherent Multiwavelength Optical Reflection Electric-driven (CMORE) spectroscopy offers investigators of condensed matter nuclear science a new diagnostic – in addition to calorimetry and detection of classic emissions. The fact that these discerning spectra occur at the beginning of an experimental run before the temperature and calorimetry can respond in both nanomaterials, and now aqueous systems as reported here, is of tremendous potential value to experimentalists because it may enable avoiding inactive modes and undesired quenching reactions.

Keywords: Anti-Stokes, CMORE spectroscopy, Excess heat mode, Lattice assisted nuclear reactions, Nickel/H_2O/Pt, Phonon gain, PHUSOR®-type component, Spectroscopy

1. Introduction

Coherent Multiwavelength Optical Reflection Electric-driven (CMORE) spectroscopy is capable of rapidly differentiating inactive and active states in CF/LANR nanomaterials and aqueous systems. Previous results include ZrO_2PdD NANOR®-type preloaded components driven in the desired, active "Excess Heat" mode, as described elsewhere [1,2]. This report expands that knowledge and shows (cf. Fig. 1) that for successful LANR in an aqueous Nickel/H_2O/Pt system containing ordinary water of natural deuteron abundance. Its "excess heat" mode is indicated by a unique signature using dual wavelength electric-driven volume-enhanced reflection spectroscopy. Shown in Fig. 1 are two spectra of the same LANR component resolved by dual wavelength CMORE spectroscopy. The two modes (responses) are the undriven "off"-state, and the optimal operational state, the "Desired Active Mode", where "excess" energy is being released. The "Excess Heat" (XSH) Mode can be distinguished in its CMORE spectra observed by a unique reflected optical backscatter along with the reflected optical beams. Note the increase of the anti-Stokes Peak from the active state of an aqueous Nickel/H_2O/Pt system.

*Mitchell R. Swartz ScD, MD, EE, E-mail: mica@theworld.com.

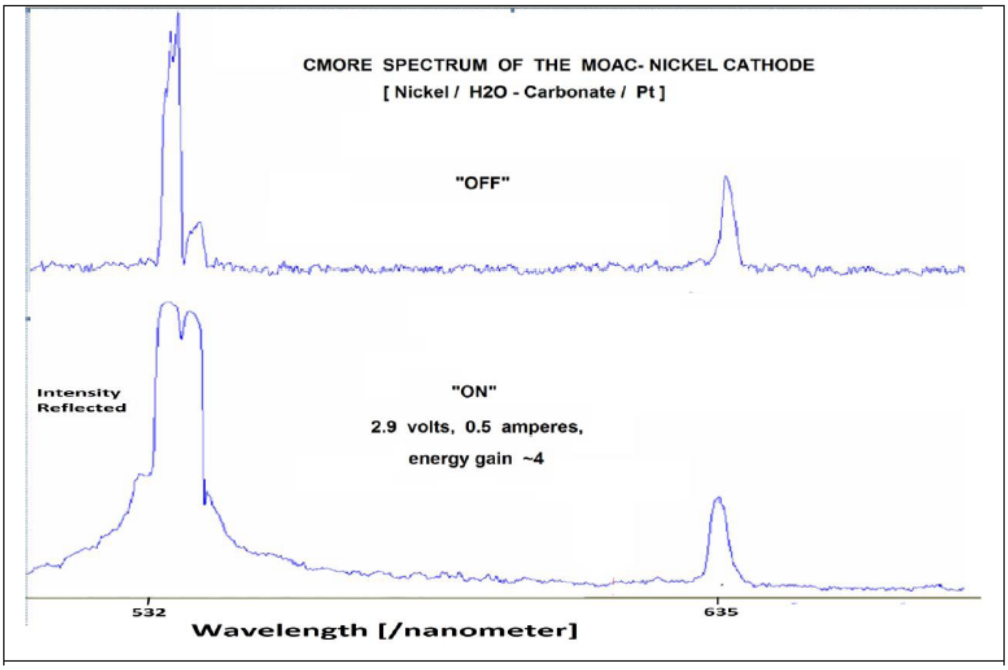

Figure 1. CMORE spectra of an aqueous Nickel/H_2O/Pt system. These are two CMORE spectra of a CF/LANR aqueous Nickel/H_2O/Pt system in two electrical states; "off" (*top*), and active XSH mode (*bottom*). Shown are the reflected optical intensities as a function of wavelength (increasing to the right-hand side).

2. Background

2.1. Successful LANR requires considerable engineering

LANR success is rewarded by "excess heat", which means that the energy producing reactions have generated de novo helium into the lattice (~10^{12} for every molecules/J [3]). There are also other reactions, but most are unwanted and many quench the desired reactions and pathways. The LANR method which Fleischmann and Pons first taught in March 1989 (aqueous, low impedance, Pd/D_2O/Pt) had problems, including inefficiency and non-reproducibility. This created havoc for those inexperienced in metallurgy, electrochemistry, and physics. Many "negative" results are due to a failure to operate the system at the optimal operating point, which is an optimum peak in the excess heat and power gain curves as a function of input electrical power [3–5].

2.2. Dry NANOR®-type CF/LANR preloaded components

Dry preloaded NANOR®-type LANR (lattice assisted nuclear reaction) components have been described in the literature [6,7]. The NANOR®-type components have been used to investigate material science [1,2,6–12] and radiation physics [1,2,10,11] of their active LANR systems. Several reports demonstrated that several electrical transconduction states exist, but that only one is active, desired, and capable of producing "excess heat" [1,2,12].

2.3. Optical Raman, and coherent Raman, scattering

Classic Raman spectroscopy involves the inelastic scattering of light which generates new frequencies which result from the interaction of light the irradiated matter [13]. Raman Stokes scattering transfers some of the energy from the incident light to excited states in the irradiated material, and thus some of the reflected wavelengths are red-shifted. Raman anti-Stokes scattering results when the irradiated material already contains excited states, and the reflected photons are blue-shifted by the difference in energy between the excited states returning to their ground state.

The major problem of the Raman effect is that it produces very weak signals because the photon conversion efficiencies are less than 10^{-18}. As Sir Chandrasekhara Raman stated, the effect has "excessive feebleness" [13]. These very small signals result because the proportionality constant $\chi(3)$, known as the "third-order susceptibility", is only linearly proportional to the local oscillator density.

However, that is not the case when irradiation is made using coherent lasers which yield a much larger signal because with coherent illumination there results phase-matching conditions and quadratic dependence on the number of local oscillators. Thus, even with the same selection rules, the coherent irradiation Raman effect yields a much greater signal intensity (circa 10^6 times greater) [14,15]. Maker and Terhune [16] first reported on Coherent Anti-Stokes Raman Scattering (CARS [17]) using a pulsed ruby laser and a Raman generated frequency-shifted beam to examine benzene. The CARS has since produced a new imaging modality for biomedicine [18,19]. Similarly, coherent anti-Stokes Raman scattering in CF/LANR (CMORE spectroscopy) has yielded a new imaging modality for excited energy states which only appear in working active CF/LANR systems [1,2].

2.4. CMORE coherent Raman scattering of CF/LANR materials

In Fig. 2, shown are the CMORE spectra which were obtained from a ZrO_2 preloaded active nanomaterial demonstrating power gain. As in Fig. 1, the spectra in Fig. 2 show reflected optical intensity as a function of wavelength, initially from two incident coherent optical beams but then reflected by backscatter along with the initial optical beams from the nanomaterial. The CMORE spectra reveal different types of activity states from the same sample, observed by the same diagnostic. Specifically, Fig. 2 shows this for the same NANOR®-type component electrically driven in three states. One state is the unwanted electrical avalanche mode [12]. The other state is the desired optimal operational state (the active excess heat (XSH) mode), where excess energy is being released. The third state is the state where the electrical drive is "off".

Note the apparent diversity in outcome of the spectra for the same input. Anti-Stokes peaks appear when the electrical drive generates excess heat but differ in energy, amount, and in what stimulates their appearance. When driven in the avalanche mode, the anti-Stokes peaks differ considerably from those which appear during the excess heat-producing or desired mode.

2.5. Dry NANOR®-type CF/LANR preloaded components

Dry preloaded NANOR®-type LANR (lattice assisted nuclear reaction) components have been described in the literature [6,7]. The NANOR®-type components have been used to investigate material science [1,2,6–12] and radiation physics [1,2,10,11] of their active LANR systems. Several reports demonstrated that several electrical transconduction states exist, but that only one is active, desired, and capable of producing "excess heat" [1,2,12].

In Fig. 2, the CMORE spectra were obtained from a ZrO_2 preloaded active nanomaterial demonstrating power gain. As with Fig. 1, the spectra in Fig. 2 show reflected optical intensity as a function of wavelength, initially from two incident coherent optical beams but then reflected by backscatter along with the initial optical beams from the nanomaterial.

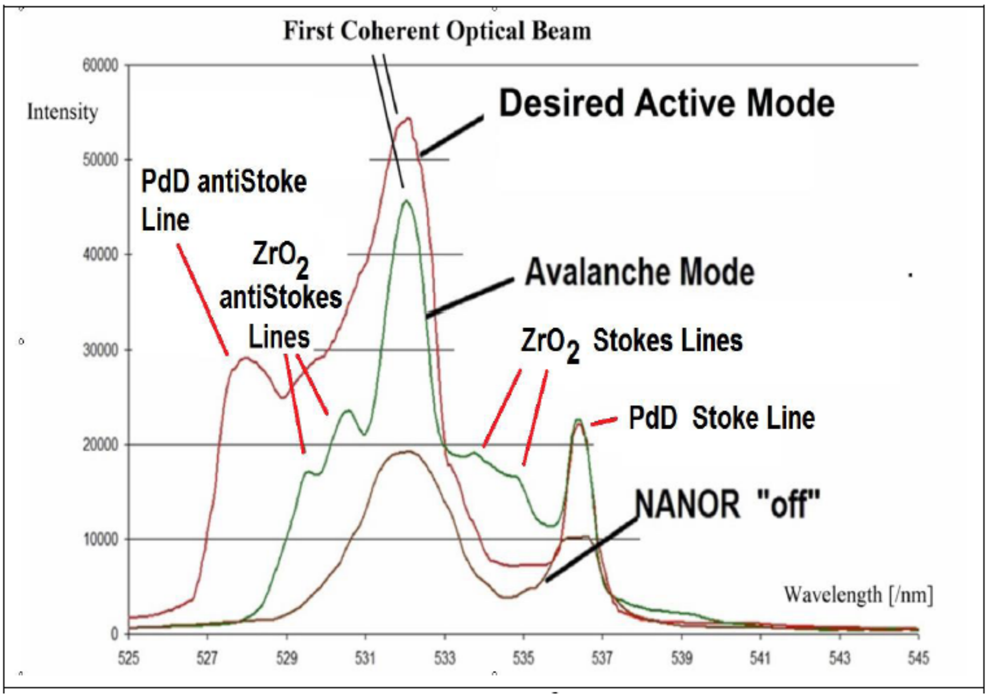

Figure 2. CMORE spectra of ZrO_2PdD NANOR®-type CF/LANR. These are the overlaid spectra of the three different electronic states optical signatures for the same preloaded ZrO_2PdD NANOR®-type CF/LANR component in three different electrical drive modes. Shown are spectra of the same NANOR®-type CF/LANR component (Nanor® 7,6) in three different electronic states, resolved by dual wavelength coherent electric-driven volume-enhanced reflection spectroscopy. Labelled are the assignments of the anti-Stokes peaks to zirconia and PdD.

The CMORE spectra reveal different types of activity states from the same sample, observed by the same diagnostic. Specifically, Fig. 2 shows this for the same NANOR®-type component electrically driven in two states (the unwanted electrical avalanche mode [12] and the optimal operational state, the desired, active XSH mode, where excess energy is being released), and "off". There is diversity and distinguishing spectra in outcome.

Anti-Stokes peaks appear when the electrical drive generates excess heat but differ in energy, amount, and in what stimulates their appearance. When driven in the avalanche mode, the anti-Stokes peaks differ considerably from those which appear during the excess heat-producing or desired mode.

3. Experimental

3.1. Materials – MOAC cell and system

The aqueous cell system used for this report is a Ni/H_2O/Pt system which was designed to have a large electrode area [20]. The cathode weighs 4.7 pounds, and was made from #46 hard drawn smooth nickel wire (0.00399 cm diameter, with an area of ~240,000 cm^2). The anode was five folded platinized sheets of titanium with an area of ~3200 cm^2, for a surface area ratio of cathode to anode of 75:1. The electrolyte was a dilute carbonate solution (K_2CO_3); ~0.1 M in distilled water of natural deuteron abundance. Two internal ohmic controls were used. Figure 3 shows the LANR cell

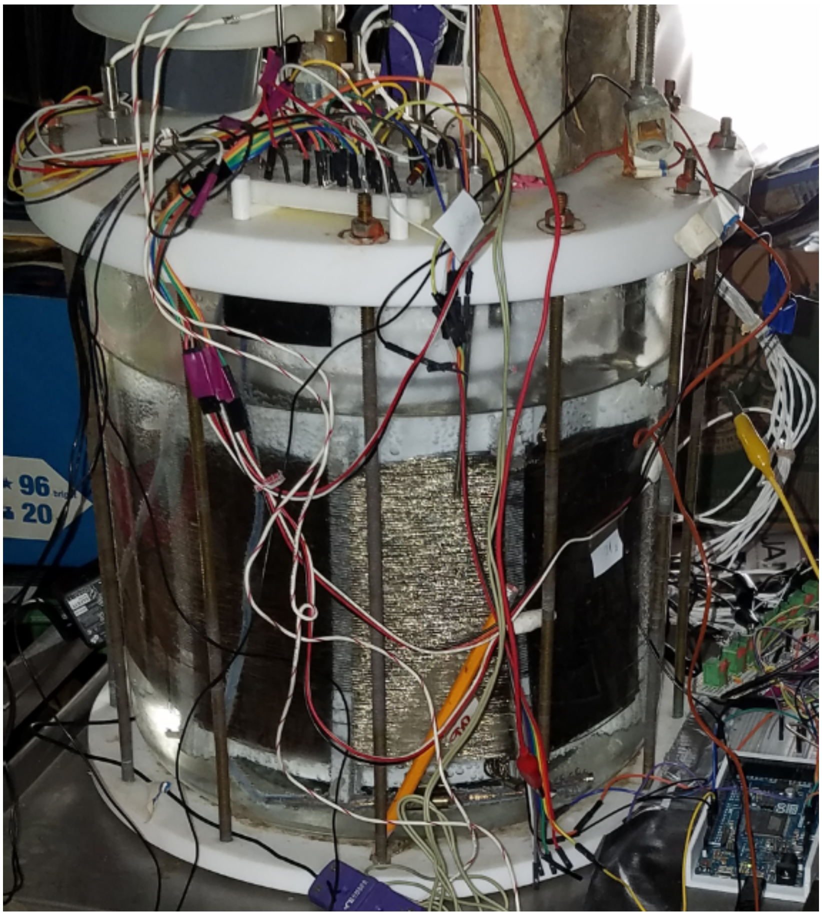

Figure 3. The LANR MOAC electrolytic cell. This figure shows the electrolytic cell used (3 l). Acquisition of the cathode surface by the CMORE spectrophotometer's incident coherent optical beam was to a small area of the very large cathode.

used. It has a 3 l capacity when filled; here unfilled, not connected to the power supply, thermistor monitoring system, or the gas venting actually used.

3.2. Methods – Signal pickup by CMORE spectroscopy

In this study, a 532 nm laser was used to elicit the Raman spectra, and a weaker 635 nm laser was used for calibration [1,2]. The green laser (532 nm peak) had a power output level of about 150 mW. The red orange laser (635 nm peak) had a power output level of about ~2 mW for energy calibration. The sample surface illuminated was the cathode.

3.3. Methods – Electrical driving components

The cell was electrical driven, or not, by a steady direct current electrical drive [2.9 V, 0.50 A; with a measured energy gain of ~4.0 using $V \times I$ as the electrical input) while it was irradiated by the two lasers while physically maintained in position. The component was electrically activated and controlled, and was designed to include and use several controls. Using several ohmic (thermal) and other controls, the anti-Stokes to Stokes (aS/S) ratio was determined when the materials were examined in both the "off" condition and where the desired cold fusion reactions occur [1,2].

4. Results

In Fig. 1, the curves are from dual wavelength coherent electric-driven volume-enhanced reflection spectroscopy of aqueous Nickel/H_2O/Pt system with power gain – and when "off". CMORE spectra show reflected optical intensity as a function of wavelength, initially from two incident coherent optical beams but then reflected by backscatter along with the initial optical beams from a small area of the electrically driven (or not) cathode.

In Fig. 1, the functional, desired "Excess Heat" (XSH) Mode is indicated by a unique signature using dual wavelength electric-driven volume-enhanced reflection spectroscopy. One can easily see the distinguishing optical output in the desired correctly driven active "state" as revealed by the new diagnostic technology.

The reflected optical backscatter along with the reflected optical beams from the component in its desired "excess heat" state has an XSH-related anti-Stokes peak which is singular and at higher energy. This distinguishing, higher energy, single, anti-Stokes peak (which also heralds phonon gain) is not seen in the "off" state.

5. Conclusions

5.1. Anti-Stokes peaks of the electrically driven Ni/H_2O–D_2O/Pt system reveals the desired "excess heat" state

The CMORE spectroscopy heralds the "desired mode" or "excess heat production mode", as demonstrated again in this report. Active aqueous Nickel/H_2O/Pt CF/LANR systems with power gain have diagnostic CMORE spectroscopic signatures. There is an XSH-related anti-Stokes peak which is singular and at higher energy. This distinguishing, higher energy, single, anti-Stokes peak (which also heralds phonon gain) is not seen in the "off" state.

From a materials point of view, it appears that acoustic phonons result from, or are required for, an active cold fusion process producing energy gain in its "excess heat" (XSH) mode in both this aqueous system and nanomaterial CF/LANR systems.

5.2. Implications for improvement of LANR systems

There are important implications to this new finding. CMORE spectroscopy is capable of rapidly differentiating the inactive or quenched states from the active excess heat (XSH) producing state in CF/LANR electrodes, nanomaterials, and systems. Successful cold fusion systems indicate their activity by a large increase in the aS/S ratio for BOTH active aqueous and nanomaterial CF/LANR systems.

Therefore, CMORE spectroscopy is a useful diagnostic which can generate spectra in real time and is able to illuminate, visualize, and help identify different states for a CF/LANR material or component, before the appearance of measurable excess heat for the first time. The system can determine which state the material or component is in, in real time, even as it is electrically driven, and may be able to determine time constants for changes between levels.

Most importantly, CMORE spectroscopy can saliently detect the desired reactions just as products begin to appear and accumulate (e.g. heat). Therefore, it has great use because it reveals both the desired, and undesired, reactions and states and may enable better control, and possible detection of other states of operation – and therefore reactions and products. For example, by observing the presence and perhaps width of the anti-Stokes peak, it may be possible to better tune CF/LANR systems away from undesired inactive modes and quenching reactions (such as the unwanted avalanche mode in CF/LANR nanomaterials).

Acknowledgments

The author acknowledges and thanks Gayle Verner for her helpful comments and editorial assistance, along with Alan Weinberg, Jeffrey Tolleson, Brian Ahern, and Charles Haldemann, Alex Frank, Joshua Gyllinsky, Florian Metzler, Charles Entenmann, Christy Frazier, Dennis Cravens, Dennis Letts, Frank Gordon, Pamela Mosier-Boss, Lawrence Forsley, David Nagel, Robert Smith, Jeff Driscoll, Jean-Paul Biberian and Louis DeChiaro. This effort was supported by JET Energy Inc. and the New Energy Foundation. NANOR® is a registered trademark of JET Energy, Incorporated. NANOR®-technology and other technology described here are protected by patents pending. PHUSOR® and NANOR® are registered trademarks of JET Energy Inc. PHUSOR® and NANOR®-technology and the technology described here are protected by patents pending.

References

[1] M.R. Swartz and P.L. Hagelstein, Increased PdD anti-Stokes peaks are correlated with excess heat mode, *J. Condensed Matter Nucl. Sci.* **24** (2017) 130–145.

[2] M.R. Swartz, Optical detection of phonon gain distinguishes an active cold fusion/LANR component, *J. Condensed Matter Nucl. Sci.* **20** (2016) 29–53.

[3] M.R. Swartz, Survey of the observed excess energy and emissions in lattice assisted nuclear reactions, *J. Sci. Exploration* **23** (4) (2009) 419–436.

[4] M.R. Swartz, Excess power gain using high impedance and codepositional lanr devices monitored by calorimetry, heat flow, and paired stirling engines, *Proc. ICCF14* **1** (2008) 123; ISBN: 978-0-578-06694-3, 123, (2010); www.iscmns.org/iccf14/ProcICCF14a.pdf.

[5] M.R. Swartz and G. Verner, Excess heat from low electrical conductivity heavy water spiral-wound Pd/D_2O/Pt and Pd/D_2O-$PdCl_2$/Pt devices, *Condensed Matter Nucl. Sci. Proc.ICCF-10*, World Scientific, Singapore, ISBN 981-256-564-6, 29-44; 45-54 (2006).

[6] [6] M.R. Swartz, G. Verner, J. Tolleson and P.L. Hagelstein, Dry, preloaded NANOR®-type CF/LANR components, *Current Science* **108** (4) (2015) 595.

[7] M.R. Swartz, G. Verner and J. Tolleson, Energy gain from preloaded ZrO_2–PdNi–D nanostructured CF/LANR quantum electronic components, *J. Condensed Matter Nucl. Sci.* **13** (2014) 528; www.iscmns.org/CMNS/JCMNS-Vol13.pdf.

[8] M.R. Swartz and P.L. Hagelstein, Demonstration of energy gain from a gain using fractionated magnetic fields on ZrO_2–PdD nanostructured preloaded ZrO_2–PdD nanostructured CF/LANR quantum electronic device at MIT, *J. Condensed Matter Nucl. Sci.* **13** (2014) 516; www.iscmns.org/CMNS/JCMNS-Vol13.pdf.

[9] M.R. Swartz, G. Verner, J. Tolleson, L. Wright, R. Goldbaum and P.L. Hagelstein, Amplification and restoration of energy components, *J. Condensed Matter Nucl. Sci.* **15**(2015) 66; www.iscmns.org/CMNS/JCMNS-Vol15.pdf.

[10] M.R. Swartz, Incremental high energy emission from a ZrO_2–PdD nanostructured quantum electronic component CF/LANR, *J. Condensed Matter Nucl. Sci.* **15**(2015) 92; www.iscmns.org/CMNS/JCMNS-Vol15.pdf.

[11] M.R. Swartz, G. Verner J. Tolleson, L. Wright, R. Goldbaum, P. Mosier-Boss and P.L. Hagelstein, Imaging of an Active NANOR®-type LANR component using CR-39, *J. Condensed Matter Nucl. Sci.* **15** (2015) 81; www.iscmns.org/CMNS/JCMNS-Vol15.pdf.

[12] M.R. Swartz, P.L. Hagelstein and G. Verner, Impact of electrical avalanche through a ZrO_2–NiD nanostructured CF/LANR component on its incremental excess power gain, ICCF-19, *J. Condensed Matter Nucl. Sci.* **19** (2016) 1–11.

[13] C.V. Raman, Scientific papers of C.V. Raman, S. Ramaseshan (Ed.), Vol. 1, India, *The Scattering of Light*, Indian Academy of Sciences, Bangalore, India, 1988.

[14] Ji-xin Cheng, Eric O. Potma and X. Sunney Xie, Coherent anti-Stokes Raman scattering correlation spectroscopy: probing dynamical processes with chemical selectivity, *J. Phys. Chem.* A **106** (2002) 8561–8568.

[15] Conor L. Evans and X. Sunney Xie, Coherent anti-Stokes Raman scattering microscopy: chemical imaging for biology and medicine, *Ann. Rev. Anal. Chem.* **1** (2008) 883–909.

[16] P.D. Maker and R.W. Terhune, Study of optical effects due to an induced polarization third order in the electric field strength, *Phy. Rev.* **137** (3A) (1965) 801–818.
[17] R.F. Begley, A.B. Harvey and R.L. Byer, Coherent anti-Stokes Raman spectroscopy, *Appl. Phys. Lett.* **25** (7) (1974) 387–390.
[18] C.L. Evans, E.O. Potma, M. Puoris'haag, D. Cote, C.P. Lin and X.S. Xie, Chemical imaging of tissue in vivo with video-rate coherent anti-Stokes Raman scattering microscopy, *Proc. Natl. Acad. Sci*. USA, **102** (2005) 16807.
[19] C.L. Evans, X. Xu, S. Kesari, X.S. Xie, S.T.C. Wong and G.S. Young, Chemically-selective imaging of brain structures with CARS microscopy, *Opt. Expr.* **15** (2007) 12076.
[20] M.R. Swartz, C. Haldemann, A. Weinberg and B. Ahern, Excess heat is linked to deuterium loss in an aqueous nickel CF/LANR system, Poster ICCF-21, and Proc. ICCF21, to appear.